Penetration by a Negatively Buoyant Vortex Ring

Takashi NAITOH, Nobuyuki OKURA, Tomomi TANAKA & Fumihito GOTO

Abstract In order to investigate the vortex motion affected by buoyancy force, we experimentally formed a negatively buoyant vortex ring by pushing less dense fluid vertically downward out of a nozzle and measured the penetration depth of it in the wide Reynolds number range, $3{,}000 < Re < 30{,}000$. We confirmed that the penetration depth of negatively buoyant vortex rings generally depends only on the Froude number and it is larger than that of the jet for the same Froude number in the range of $Fr > 2$. The formation conditions of buoyant vortex rings to be turbulent or laminar are also examined, since the characteristic features of buoyant turbulent vortex rings are markedly different from those of buoyant laminar rings.

1 Introduction

The dynamic behavior of vortex rings affected by buoyancy force is of inherent interest not only with respect to atmospheric phenomena but also in engineering applications such as environmental problems. Since the motion of a vortex ring is relatively stable and it can be translated over a long distance due to the self-induced velocity, it has been employed to study the characteristic features of vortex motion, such as interaction of a vortex with another vortex (e. g., merging, pairing, mutual slip-through) and interaction of a vortex with a solid body[1-3]. In this paper, by the use of vortex rings formed by pushing lighter fluid vertically downward out of a nozzle, we investigate the vortex motion affected by negative buoyancy force.

Takashi NAITOH
Nagoya Institute of Technology, Gokiso-cho, Showa-ku, Nagoya, 466-8555, Japan,
e-mail: naitoh.takashi@nitech.ac.jp

Nobuyuki OKURA
Meijo University, 1-501 Shiogamaguchi, Tempaku-ku, Nagoya 468-8502, Japan,
e-mail: ohkura@meijo-u.ac.jp

A buoyant vortex ring can be classified as positively and negatively buoyant, depending on the direction of the buoyancy force and momentum flux of ejected fluid. In the case of positively buoyant vortex rings, Turner (1957) [4] analyzed the motion of buoyant vortex rings by assuming that the circulation remains constant and the impulse increases owing to the buoyant force in the far field. Bond and Johari (2010) [5] examined the development of a positively buoyant vortex ring in the near field experimentally with LIF and PIV measurements. Flow visualization and some quantitative experiments for this kind of vortex rings were also conducted on small-scale simulated microbursts[6,7].

In the case of negatively buoyant vortex rings, several papers have examined the motion of vortex rings generated in a starting jet [8-12]. Myrtroeen et al. [12] studied the combined effect of buoyancy and dimensionless piston stroke on the maximum rise height of heavy fluid injected upward from inside a cylinder. Since the buoyancy force decelerates the velocity of the vortex ring, special interest has been paid to the penetration depth (or the rise height) of these non-homogeneous jets and rings, and these lengths are found to be dependent only on the Froude number, $\mathrm{Fr} = U_j \Big/ \sqrt{g(\rho_{amb} - \rho_j) D_O / \rho_{amb}}$, where U_j is the fluid ejection velocity, g is gravitational acceleration, (ρ_{amb} - ρ_j) is the difference in density between the ambient and the ejected fluid, and D_O is the diameter of the nozzle.

However, these studies are carried out within a small range of Reynolds numbers, Re = $U_j D_O/\nu$, Re = 1000 to 3000. In several industrial applications and in nature, however, vortex rings for Reynolds numbers several times larger than this range should be examined. Therefore, in the present study, we investigate primarily the maximum penetration depth of a negatively buoyant vortex ring over a wide range of Reynolds numbers, 3000 < Re < 30000.

2 Experimental apparatus

We used two size of the water tanks with dimensions of 300 mm L × 300 mm W × 700 mm H and 300 mm L × 600 mm W × 1200 mm H. A vortex ring generator which consists of a piston-cylinder mechanism and a nozzle is fixed at the center of the open surface of the tank. The vortex rings are generated by pushing the fluid inside the cylinder via a piston. A linear motor (LAS 4B 500AW, Oriental Motor) configured by a stepping motor and rack-and-pinion mechanism

drives the piston. The movement of the piston is controlled by pulse signals generated by an embedded microcomputer.

In order to produce enough momentum of a vortex ring, small nozzles ranging from 20.0 mm to 40.0 mm diameter and two size of piston diameters (D_p = 70 mm, 120mm) were used for all the experiments. The outer contour of the cylindrical nozzle was shaped to form a wedge with a tip angle of 45 degrees so as not to prevent the rolling up.

3 Transition map

The characteristic features of buoyant turbulent vortex rings are markedly different from those of buoyant laminar rings. Then it is important to investigate the formation conditions of buoyant vortex rings to be turbulent or laminar. Note that most of the negatively buoyant vortex ring generated by the present formation conditions becomes turbulent, whereas that in the literature [8 - 12] might be laminar. According to Glezer (1988) [13], vortex rings at $Re_\Gamma < 2.0 \times 10^4$ with a small jet length-to-diameter ratio, $L_O/D_O = 2$ generated in a homogeneous fluid remain laminar until the azimuthal wavy deformation appears, where Re_Γ is defined by the ratio of the circulation of a vortex ring to the kinematic viscosity ν. However, for the case of a non-homogeneous fluid, the vortex ring at $Re_\Gamma < 2.0 \times 10^4$ becomes turbulent because of fluid ejection from the vortex ring and Rayleigh-Taylor instability. Figure 1 shows the successive cross sections of the vortex ring at $L_O/D_O = 2$ for $Re_{\Gamma slug} = 9000$ and Fr = 7.2 by using planar laser induced fluorescence. Here, $Re_{\Gamma slug}$ is defined by the ratio of the circulation of a vortex ring estimated based on the slug model [1] to the kinematic viscosity ν. When the shear layer separated from the nozzle tip is rolling up, the spiral streak lines are distorted due to Rayleigh-Taylor instability, because ambient dense fluid is entrained into a vortex ring which is consisted of lighter fluid with spirals in the process of vortex formation as shown in Fig. 1 (a). Subsequently the state of the ring becomes laminar once from t = 1.0 s to 3.0 s judging from the orderly streak lines. However, after that the spiral streak lines are blurred and distorted at about t = 4.0 s, then the ring becomes turbulent.

The vortex rings generated by the same formation condition except for the Froude number are presented in Fig. 2 and Fig. 3. The effect of Rayleigh-Taylor instability grows and the period being

laminar is shorten as Fr decreases. The transition to turbulence is seen at about $t = 1.5$ s in Fig. 2. For the case of Fr = 2.6 observed in

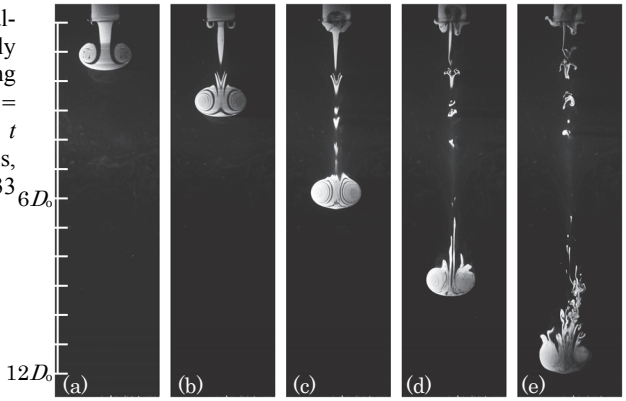

Fig. 1 Successive visualization of negatively buoyant vortex ring ($Re_{\Gamma slug}$ = 9000, Fr = 7.2): (a) t = 0.67 s, (b) t = 1.33 s, (c) t = 2.67 s, (d) t = 4.00 s, (e) t = 5.33 s.

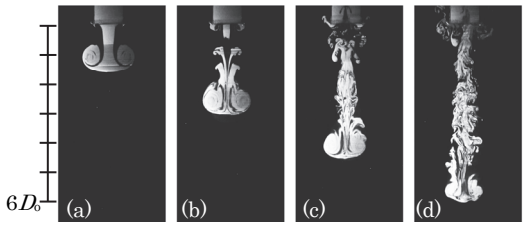

Fig. 2 Successive visualization of negatively buoyant vortex ring ($Re_{\Gamma slug}$ = 9000, Fr = 3.6): (a) t = 0.67 s, (b) t = 1.33 s, (c) t = 2.00 s, (d) t = 2.67 s.

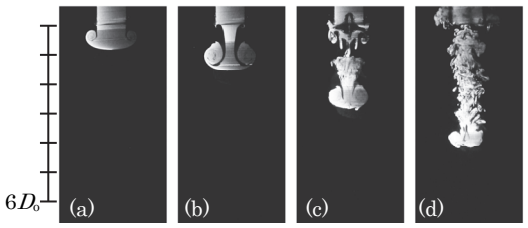

Fig. 3 Successive visualization of negatively buoyant vortex ring ($Re_{\Gamma slug}$ = 9000, Fr = 2.6): (a) t = 0.33 s, (b) t = 0.67 s, (c) t = 1.33 s, (d) t = 2.00 s.

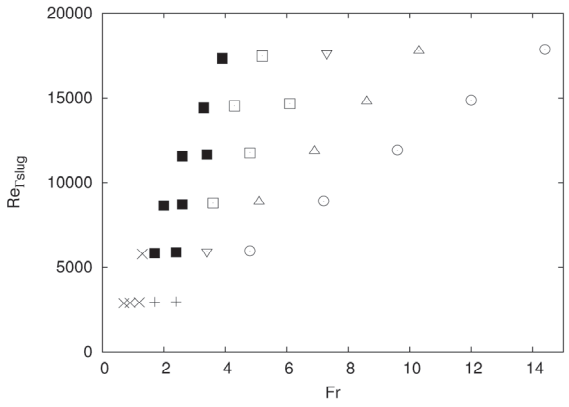

Fig. 4 Transition map of the negatively buoyant vortex ring at $Lo/Do = 2.0$.: filled squares, $x_t/Do < 2$; open squares, $2 < x_t/Do < 4$; down-pointing triangles, $4 < x_t/Do < 6$; triangles, $6 < x_t/Do < 8$; open circles, $8 < x_t/Do < 10$; crosses, no vortex ring is formed at all; plus signs, a vortex ring that keeps laminar until it stops moving.

Fig. 3, the turbulent vortex ring appears just after the ring formation and the laminar state can't be observed.

Figure 4 shows the transition map of the negatively buoyant vortex ring at $L_0/D_0 = 2$. These data are classified by the states of vortex ring. Here, x_t is defined as the position where the transition to turbulence occurs. It is worth noting that the transition of vortex rings depends on both Froude number and Reynolds number.

4 Penetration depth

Figure 5 shows the maximum penetration depth of negatively buoyant vortex rings and jets. Although the scatter of the data is not small, the trend of the penetration depth of the vortex rings with respect to the Froude number can be determined. Fitting a line to the penetration depth yields the equation $z/D_0 = 8.8\ \mathrm{Fr} - 13.3$ (Fr > 2). The plotted symbols are changed according to the Reynolds number and the trend of the penetration depth with respect to the Reynolds number is examined. However, the dependency of these data on the Reynolds number cannot be identified.

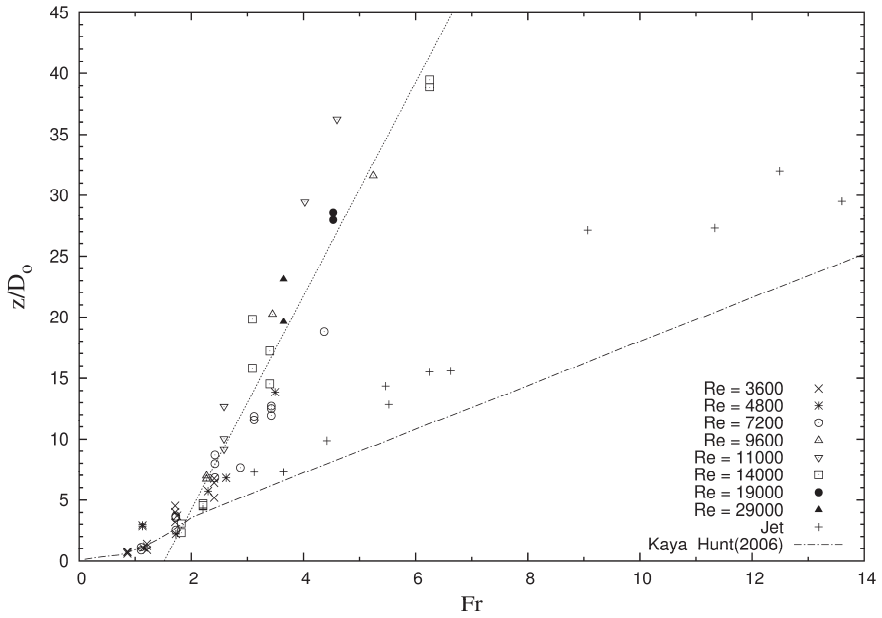

Fig. 5 Maximum penetration depth of the negatively buoyant vortex ring and jet.

The "+" symbol represents the initial penetration depth of jets generated in the same apparatus, and the dot-dashed line shows the fitting equation of the penetration depth of jets in a steady state reported by Kaye and Hunt [14]. Turner [15] presented experimental results that showed the initial rise height is larger than the steady-state rise height. Therefore, it is reasonable that the data denoted by "+" exceed the dot-dashed line.

Based on these results, the Reynolds number is confirmed to have an insignificant effect on the penetration depth of negatively buoyant vortex rings, regardless of the wide Re range, $3{,}000 < Re < 30{,}000$, and the penetration depth of the negatively buoyant vortex ring is larger than that of the jet for the same Froude number in the range of $Fr > 2$.

References

1. T. T. Lim and T. B. Nickels, *Fluid Vortices* (Kluwer Academic Publishers, Dordrecht, 1995), pp. 95–149.
2. K. Shariff and A. Leonard, "Vortex rings," Annu. Rev. Fluid Mech. **24**, 235 (1992).
3. P. G. Saffman, *Vortex Dynamics* (Cambridge University Press, Cambridge, 1992).
4. J. S. Turner, "Buoyant vortex rings," Proc. Roy. Soc. London A 239 (1957) pp. 61-75.
5. D. Bond and H. Johari, "Impact of buoyancy on vortex ring development in the near field," Exp. in Fluids 48 (2010) pp. 737-745.
6. Alahyari and E. K. Longmire, "Particle image velocimetry in a variable density flow: application to a dynamically evolving microburst," Exp. in Fluids, 17 (1994) pp. 434-4340.
7. T. S. Lundgren, J. Yao, and N. N. Mansour, "Microburst modelling and scaling," J. Fluid Mech. 239 (1992) pp. 461-488.
8. Ruo-Qian Wang, Adrian Wing-Keung Law, E. Eric Adams, and Oliver B. Fringer. Buoyant formation number of a starting buoyant jet. *Phys. Fluids*, **21**:125104, 2009.
9. Ruo-Qian Wang, Adrian Wing-Keung Law, and E. Eric Adams. Pinch-off and formation number of negatively buoyant jets. *Phys. Fluids*, **23**:052101, 2011.
10. C. Marugán-Cruz, J. Rodríguez-Rodríguez, and C. Martínez-Bazán. Negatively buoyant starting jets. *Phys. Fluids*, **21**:117101, 2009.
11. C. Marugán-Cruz, J. Rodríguez-Rodríguez, and C. Martínez-Bazán. Formation regimes of vortex rings in negatively buoyant starting jets. *J. Fluid Mech.*, **716**:470–486, 2013.
12. O. J. Myrtroeen and G. R. Hunt. Negatively buoyant projectiles – from weak fountains to heavy vortices. *J. Fluid Mech.*, **657**:227–237, 2010.
13. A. Glezer. The formation of vortex rings. Phys. Fluids, 31: 3532-3542, 1988.
14. N. B. Kaye and G. R. Hunt. Weak fountains. *J. Fluid Mech.*, **558**:319–328, 2006.
15. J. S. Turner. Jets and plumes with negative or reversing buoyancy. *J. Fluid Mech.*, **26**:779–792, 1966.